

# Robust MPC Based on Multivariable RBF-ARX Model for Nonlinear Systems

Hui Peng, Weihua Gui, Kazushi Nakano, and Hideo Shioya, *Member, IEEE*

**Abstract**—For a class of smooth nonlinear multivariable systems whose working-points vary with time and which may be represented by a linear MIMO ARX model at each working-point, a combination of a local linearization and a polytopic uncertain linear parameter-varying (LPV) state-space model are built to approximate the present and the future system's nonlinear behavior respectively. The combination models are constructed on the basis of a matrix polynomial MIMO RBF-ARX model identified offline for characterizing the underlying nonlinear system. A min-max robust MPC strategy is investigated for the systems based on the approximate models proposed. The closed loop stability of the MPC algorithm is guaranteed by the use of time-varying parameter-dependent Lyapunov function and the feasibility of the linear matrix inequalities (LMIs). The effectiveness of the modeling and control methods proposed in this paper is illustrated by a case study of a thermal power plant simulator.

## I. INTRODUCTION

Nonlinear model predictive control (NMPC) has been the object of extensive study in recent years, and the theory related to stability and optimality has reached a point of relative maturity, as outlined in [8]. In many reports on the research and application of NMPC, the control schemes [1][2] were based on the direct use of nonlinear models, but they involved the on-line solution of a higher order nonlinear optimization problem with constraints, which is usually computationally expensive and may be even unable to guarantee to get a feasible solution in real time control. Another kind of approach used a piecewise linearization technique [3][4] or a polytopic uncertain LPV (linear parameter varying) model [5][6][7] to describe the nonlinear behavior of a system, so that the model was linearized in each sampling interval. This resulted in the solution of one or more quadratic programming problems or LMIs (linear matrix inequalities) at each such interval, as in case of linear MPC. Nevertheless, the identification experiment of many linear

This work was supported by the National Natural Science Foundation of China under Grant 60443008 and by the Institute of Statistical Mathematics, Tokyo, Japan.

Hui Peng is with the School of Information Science & Engineering, Central South University, Changsha, Hunan, 410083, China ( phone: +86-731-8830642; fax: +86-731-8830642; e-mail: huipeng@mail.csu.edu.cn).

Weihua Gui is with the School of Information Science & Engineering, Central South University, Changsha, Hunan, 410083, China ( e-mail: gwh@mail.csu.edu.cn).

Kazushi Nakano is with the Department of Electronic Engineering, the University of Electro-Communications, 1-5-1 Chofu-ga-oka, Chofu, Tokyo 182-8585, Japan (e-mail: nakano@ee.uec.ac.jp).

Hideo Shioya is with Bailey Japan Co. Ltd., 511 Baraki, Nirayama-cho, Tagata-gun, Shizuoka, 410-2193, Japan (e-mail: hshioya@bailey.co.jp).

models that are valid only in each small region is not an easy work in practice. Besides, the NMPC designs based on an on-line estimated affine model representing a nonlinear plant, such as the quasi-linear autoregressive model [9], were also reported. However, fast and accurate online estimation of a complicated model providing a good fit to a nonlinear process may be difficult in real application.

For a class of smooth nonlinear SISO system whose working-point changes with time and its dynamic behavior may be represented by a linear model at each working-point, the SISO RBF-ARX model and its parameter optimization method [10] was proposed in order to effectively characterize such nonlinear systems. The SISO RBF-ARX model is a kind of hybrid pseudo-linear time-varying model that is composed of Gaussian radial basis function (RBF) neural networks and linear ARX model structure. The offline identified SISO RBF-ARX model-based nonlinear MPC has been investigated both in simulation and in real industrial application [11][12][13][14] where the satisfactory nonlinear modeling accuracy and significant effectiveness and feasibility of the proposed NMPC were verified. Besides, some stability conclusions on the proposed NMPC were also given in [12][13]. Furthermore, the MIMO RBF-ARX model built on the basis of the idea of SISO RBF-ARX model was also proposed in [15] to characterize a class of smooth nonlinear MIMO systems.

This paper presents an integrated modeling and robust MPC approach for the MIMO nonlinear systems on the basis of the MIMO RBF-ARX modeling technique. First, the nonlinear system is identified off-line by a MIMO RBF-ARX model. From the model, a local linearization state-space model is obtained to represent the current behavior of the nonlinear system, and a polytopic uncertain LPV state-space model is built to approximate the future system's nonlinear behavior. Subsequently, based on two approximate models, a min-max robust MPC algorithm with constraint is designed for the MIMO nonlinear systems. The closed loop stability of the MPC strategy is guaranteed by the use of parameter-dependent Lyapunov function and the feasibility of the linear matrix inequalities. Case study to a thermal power plant simulator demonstrates the effectiveness of the integrated modeling and robust MPC approach proposed.

## II. NONLINEAR SYSTEM APPROXIMATION BY MIMO RBF-ARX MODEL

Consider a MIMO nonlinear system

$$y(t+1) = f(w(t)) \quad (1)$$

$$w(t) = \begin{bmatrix} y(t)^T & \cdots & y(t-k_a+1)^T & u(t)^T & \cdots & u(t-k_b+1)^T \end{bmatrix}^T \quad (2)$$

where  $y(t) \in \mathbb{R}^n$  is the output,  $u(t) \in \mathbb{R}^m$  is the input. If the function  $f(\bullet)$  in (1) is continuously differentiable at an arbitrary equilibrium point, nonlinear system (1) may be then approximated by the following MIMO RBF-ARX model [15]

$$\left\{ \begin{array}{l} y(t+1) = \phi_0(w(t)) + \sum_{i=0}^{k_a-1} \phi_{y,i}(w(t))y(t-i) \\ \quad + \sum_{i=0}^{k_b-1} \phi_{u,i}(w(t))u(t-i) + \xi(t+1) \\ \phi_0(w(t)) = c_0^0 + \sum_{k=1}^h c_k^0 \exp\left\{-\|w(t) - z_{y,k}\|_{\lambda_{y,k}}^2\right\} \\ \phi_{j,i}(w(t)) = c_{i,0}^j + \sum_{k=1}^h c_{i,k}^j \exp\left\{-\|w(t) - z_{j,k}\|_{\lambda_{j,k}}^2\right\} \\ z_{j,k} = \begin{bmatrix} z_{j,k,1} & z_{j,k,2} & \cdots & z_{j,k,\dim(w)} \end{bmatrix}^T, j = y, u \end{array} \right. \quad (3)$$

where  $k_a$ ,  $k_b$ , and  $h$  are the orders;  $z_{j,k}$ s are the centers of Gaussian RBF networks;  $c_{i,k}^j$ s and  $c_k^0$ s are the weighting coefficient matrices of suitable dimensions;  $\|x\|_{\hat{\lambda}}^2 \triangleq x^T \hat{\lambda} x$ ,  $\hat{\lambda} = \text{diag}(\hat{\lambda}_1^2 \ \hat{\lambda}_2^2 \ \cdots \ \hat{\lambda}_{\dim(x)}^2)$ , and  $\{\hat{\lambda}_1, \hat{\lambda}_2, \dots, \hat{\lambda}_{\dim(x)}\}$  are the scaling factors;  $\xi(t) \in \mathbb{R}^n$  denotes noise usually regarded as Gaussian white noise independent of the observations. More generally, the signal  $w(t)$  in (3) could be a process variable causing the operating-point of the system to change with time.  $w(t)$  has direct or indirect relation with input or output of the system, in some cases probably being just the input or/and output itself. For example, in a nonlinear thermal power plant,  $w(t)$  may be the load demand of the plant.

MIMO RBF-ARX model (3) is constructed as a global model, and is estimated off-line from observation data so as to avoid the potential problem caused by the failure of on-line parameter estimation during real time control. It is easy to see that the local linearization of model (3) is a linear ARX model at each working-point by fixing  $w(t)$  at time  $t$  in (3). It is natural and appealing to interpret model (3) as a locally linear ARX model in which the evolution of the process at time  $t$  is governed by a set of AR coefficient matrices  $\{\phi_{y,i}, \phi_{u,i}, \phi_{v,i}\}$ , and a local mean  $\phi_0$ , all of which depend on the ‘working-point’ of the process at time  $t$ . Model (3) treats a nonlinear process by splitting the state space up into a large number of small segments, and regarding the process as locally linear within each segment. Because of the satisfactory properties of RBF networks in function approximation as well as in learning local variation, the use of the working-point dependent functional coefficient matrices makes the MIMO RBF-ARX model capable of effectively representing the dynamic characteristics of the system at each working-point. The MIMO RBF-ARX model incorporates the advantages of the state-dependent ARX model in nonlinear dynamics description and the RBF network in

function approximation. In general, the model does not need many RBF centers compared with a single RBF network model, because the complexity of the model is dispersed into the lags of the autoregressive parts of the model [10][14][15]. The MIMO RBF-ARX model may be estimated by the structured nonlinear parameter optimization method (SNPOM) [15].

It is easy to rewrite model (3) as the following matrix polynomial form:

$$y(t+1) = \sum_{i=0}^{k_n-1} a_{i+1,t} y(t-i) + \sum_{i=1}^{k_n-1} b_{i+1,t} u(t-i) + \phi_{0,t} + \xi(t+1) \quad (4)$$

where

$$\begin{aligned} k_n &= \max\{k_a, k_b\}, \quad \phi_{0,t} = \phi_0(w(t)) \\ a_{i,t} &= \begin{cases} c_{i,0}^y + \sum_{k=1}^h c_{i,k}^y \exp\left\{-\|w(t) - z_{y,k}\|_{\lambda_{y,k}}^2\right\}, & i \leq k_a \\ 0, & i > k_a \end{cases} \\ b_{i,t} &= \begin{cases} c_{i,0}^u + \sum_{k=1}^h c_{i,k}^u \exp\left\{-\|w(t) - z_{u,k}\|_{\lambda_{u,k}}^2\right\}, & i \leq k_b \\ 0, & i > k_b \end{cases} \end{aligned} \quad (5)$$

Let  $y_r \in \mathbb{R}^n$  be the desired output, and define the deviation variables below

$$\begin{cases} \bar{y}(t+i) = y(t+i) - y_r, & i = 1, -1, -2, \dots \\ \bar{u}(t+j) = u(t+j) - u(t+j-1), & j = 0, -1, -2, \dots \end{cases} \quad (6)$$

From (4) and (6), we may obtain the prediction of the output deviation,  $\bar{y}(t+1|t)$ , given by

$$\bar{y}(t+1|t) = \sum_{i=0}^{k_n-1} a_{i+1,t} \bar{y}(t-i) + \sum_{i=0}^{k_n-1} b_{i+1,t} \bar{u}(t-i) + \psi_t \quad (7)$$

$$\psi_t = -y_r + \sum_{i=0}^{k_n-1} a_{i+1,t} y_r + \sum_{i=0}^{k_n-1} b_{i+1,t} u(t-i-1) + \phi_{0,t} \quad (8)$$

The norm of  $\psi_t$ , defined by (8), i.e.  $\|\psi_t\|$ , may be regarded as an index of describing whether the system goes into steady state, because  $\|\psi_t\|$  should be zero if the input  $\{u(t)\}$  is perfect and the output  $\{y(t)\}$  is stabilized on  $y_r$  under steady state. In terms of the meaning of  $\psi_t$ , and from (7) one may use the following linear time-varying model (9) to approximate the future nonlinearities of the system and to make  $\|\psi_{t+j|t}\|$  be zero by designing a set of ‘perfect’ inputs  $\{\bar{u}(t|t), \bar{u}(t+1|t), \bar{u}(t+2|t), \dots\}$ :

$$\bar{y}(t+j+1|t) = \sum_{i=0}^{k_n-1} a_{i+1,t+j} \bar{y}(t+j-i|t) + \sum_{i=0}^{k_n-1} b_{i+1,t+j} \bar{u}(t+j-i|t) \quad (9)$$

$$\text{where } \begin{cases} \bar{y}(t+j-i|t) = \bar{y}(t+j-i), & j \leq i \\ \bar{u}(t+j-i|t) = \bar{u}(t+j-i), & j \leq i \end{cases}$$

From (5), one can see that the elements of the coefficient matrices  $a_{i,t+j}$  and  $b_{i,t+j}$  in model (9) could not be obtained at time  $t$ , because the future values of  $w(t)$  representing the working-point state usually could not be utilized, but their varying zones of the future values of  $a_{i,t+j}$  and  $b_{i,t+j}$  could be

known from (5). From matrix polynomial model (7) and (9), two state-space models (observer-canonical form) can be built by defining the state vector given below:

$$\begin{cases} x(t+j|t) = \begin{bmatrix} x_{1,t+j|t}^T & x_{2,t+j|t}^T & \cdots & x_{k_n,t+j|t}^T \end{bmatrix}^T \\ x_{1,t+j|t} = \bar{y}(t+j|t) \\ x_{k_n,t+j|t} = \sum_{i=1}^{k_n+1-k} a_{i+k-1,t+j-1} \bar{y}(t+j-i|t) \\ \quad + \sum_{i=1}^{k_n+1-k} b_{i+k-1,t+j-1} \bar{u}(t+j-i|t) \\ k = 2, 3, \dots, k_n; j = 0, 1, 2, \dots \end{cases} \quad (10)$$

The state space models corresponding to model (7) and (9) can be then respectively given by

$$\begin{cases} x(t+1|t) = A_t x(t|t) + B_t \bar{u}(t|t) + \Xi(t) \\ A_t = \begin{bmatrix} a_{1,t} & 1 & 0 & \cdots & 0 \\ a_{2,t} & 0 & 1 & \cdots & \vdots \\ \vdots & \vdots & \vdots & \ddots & 0 \\ a_{k_n-1,t} & 0 & 0 & \cdots & 1 \\ a_{k_n,t} & 0 & 0 & \cdots & 0 \end{bmatrix}, B_t = \begin{bmatrix} b_{1,t} \\ b_{2,t} \\ \vdots \\ b_{k_n,t} \end{bmatrix} \\ \Xi(t) = [\psi_t^T \ 0 \ \cdots \ 0]^T \end{cases} \quad (11)$$

and

$$\begin{cases} x(t+j+1|t) = A_{t+j|t} x(t+j|t) + B_{t+j|t} \bar{u}(t+j|t) \\ A_{t+j|t} = \begin{bmatrix} a_{1,t+j|t} & 1 & 0 & \cdots & 0 \\ a_{2,t+j|t} & 0 & 1 & \cdots & \vdots \\ \vdots & \vdots & \vdots & \ddots & 0 \\ a_{k_n-1,t+j|t} & 0 & 0 & \cdots & 1 \\ a_{k_n,t+j|t} & 0 & 0 & \cdots & 0 \end{bmatrix}, B_{t+j|t} = \begin{bmatrix} b_{1,t+j|t} \\ b_{2,t+j|t} \\ \vdots \\ b_{k_n,t+j|t} \end{bmatrix} \\ j \geq 1 \end{cases} \quad (12)$$

Notice that the state  $x(t|t)$ ,  $\Xi(t)$  and the state-matrices  $[A_t, B_t]$  in (11) can be obtained by (5), (8), (10) and (11) on the basis of the measured input/output data and the offline estimated MIMO RBF-ARX model (4). Furthermore, according to RBF-ARX model (4-5) and model (12), it can be shown that the future state-matrices  $[A_{t+j|t}, B_{t+j|t}]$  ( $j \geq 1$ ) in (12) belong to two convex polytopic sets respectively, which are given by

$$\Omega_A := \left\{ A_{t+j|t} : A_{t+j|t} = \sum_{i=1}^{L_h} \alpha_i(t+j|t) A_i, \right. \quad (13)$$

$$\left. \sum_{i=1}^{L_h} \alpha_i(t+j|t) = 1, \alpha_i(t+j|t) \geq 0 \right\}$$

$$\Omega_B := \left\{ B_{t+j|t} : B_{t+j|t} = \sum_{i=1}^{L_h} \beta_i(t+j|t) B_i, \right. \quad (14)$$

$$\left. \sum_{i=1}^{L_h} \beta_i(t+j|t) = 1, \beta_i(t+j|t) \geq 0 \right\}$$

where  $L_h = 2^h$ ;  $h = 1, 2, \dots$

$$A_{j(j=1,2,\dots,L_h)} = \begin{bmatrix} c_{0,0}^y + \sum_{i=1}^h c_{0,i}^y (\bar{e}_{y,i} | \underline{e}_{y,i}) & 1 & 0 & \cdots & 0 \\ c_{1,0}^y + \sum_{i=1}^h c_{1,i}^y (\bar{e}_{y,i} | \underline{e}_{y,i}) & 0 & 1 & \cdots & \vdots \\ \vdots & \vdots & \vdots & \ddots & 0 \\ c_{k_n-2,0}^y + \sum_{i=1}^h c_{k_n-2,i}^y (\bar{e}_{y,i} | \underline{e}_{y,i}) & 0 & 0 & \cdots & 1 \\ c_{k_n-1,0}^y + \sum_{i=1}^h c_{k_n-1,i}^y (\bar{e}_{y,i} | \underline{e}_{y,i}) & 0 & 0 & \cdots & 0 \end{bmatrix}$$

$$B_{j(j=1,2,\dots,L_h)} = \begin{bmatrix} c_{0,0}^u + \sum_{i=1}^h c_{0,i}^u (\bar{e}_{u,i} | \underline{e}_{u,i}) \\ c_{1,0}^u + \sum_{i=1}^h c_{1,i}^u (\bar{e}_{u,i} | \underline{e}_{u,i}) \\ \vdots \\ c_{k_n-1,0}^u + \sum_{i=1}^h c_{k_n-1,i}^u (\bar{e}_{u,i} | \underline{e}_{u,i}) \end{bmatrix}$$

$$(\bar{e}_{y,i} | \underline{e}_{y,i}) \triangleq \bar{e}_{y,i} \text{ or } \underline{e}_{y,i}$$

$$\bar{e}_{y,i} = \max \left\{ \exp \left( - \|w(t) - z_{y,i}\|_{\lambda_{y,i}}^2 \right), \forall w(t) \right\}$$

$$\underline{e}_{y,i} = \min \left\{ \exp \left( - \|w(t) - z_{y,i}\|_{\lambda_{y,i}}^2 \right), \forall w(t) \right\}$$

$$(\bar{e}_{u,i} | \underline{e}_{u,i}) \triangleq \bar{e}_{u,i} \text{ or } \underline{e}_{u,i}$$

$$\bar{e}_{u,i} = \max \left\{ \exp \left( - \|w(t) - z_{u,i}\|_{\lambda_{u,i}}^2 \right), \forall w(t) \right\}$$

$$\underline{e}_{u,i} = \min \left\{ \exp \left( - \|w(t) - z_{u,i}\|_{\lambda_{u,i}}^2 \right), \forall w(t) \right\}$$

In summary, a local linear model (11) is obtained to describe the current nonlinear dynamics, and the future nonlinear behavior is assumed to vary within a region constructed by an uncertain linear parameter time-varying model (12) whose dynamic matrix  $A_{t+j|t}$  belongs to  $\Omega_A$  in (13) and  $B_{t+j|t}$  is in the convex polytope  $\Omega_B$  in (14). In the next section, we give the formulations of a min-max MPC algorithm based on those models.

### III. MIN-MAX MPC ALGORITHM

MPC consists of a step-by-step optimization technique. At each step new measurements are obtained and a cost function depending on the predicted future states of the plant is minimized. Consider the following robust performance objective:

$$\begin{aligned} & \min_{\bar{u}(t|t), \bar{u}(t+j|t), j=1, 2, \dots, L_h} \max_{A_{t+j|t} \in \Omega_A, B_{t+j|t} \in \Omega_B} J_\infty(t) \\ & \text{s.t. (11), (12), } -\Delta \underline{u} \leq \bar{u}(t+i|t) \leq \Delta \bar{u}, i \geq 0 \end{aligned} \quad (15)$$

with

$$J_\infty(t) = x(t|t)^T W x(t|t) + \bar{u}(t|t)^T R \bar{u}(t|t) + J_\infty^1(t) \quad (16)$$

$$J_\infty^1(t) = \sum_{j=1}^\infty \{x(t+j|t)^T W x(t+j|t) + \bar{u}(t+j|t)^T R \bar{u}(t+j|t)\} \quad (17)$$

where  $W \geq 0$  and  $R > 0$  are suitable weighting matrices. The control input  $\bar{u}(t|t)$  in (16) is a free control move and is the first computed move that gets implemented on the plant. The rest of the future control moves are given by a state feedback:

$$\bar{u}(t+j|t) = F(t)x(t+j|t), j \geq 1 \quad (18)$$

We provide an LMI synthesis procedure for the infinite-horizon MPC problem (15). This LMI formulation is achieved by defining a quadratic function:

$$V(j,t) = x(t+j|t)^T P(j,t)x(t+j|t), j \geq 1 \quad (19)$$

where  $\forall t \geq 0$ ,  $\forall j \geq 1$ ,  $P(j,t) > 0$ . If the objective function (15) is well defined, we can state that  $V(\infty,t) = 0$  because  $x(\infty|t) = 0$ . In view of this, we impose a bound on the cost function  $J_\infty^1(t)$  by the following design requirement:

$$\begin{aligned} V(j+1,t) - V(j,t) &\leq \\ -\{x(t+j|t)^T W x(t+j|t) + \bar{u}(t+j|t)^T R \bar{u}(t+j|t)\}, \quad (20) \\ \forall A_{t+j|t} \in \Omega_A, \quad \forall B_{t+j|t} \in \Omega_B, \quad j \geq 1 \end{aligned}$$

By summing (20) for  $j=1$  to  $\infty$ , we obtain the following constraint:

$$\max_{A_{t+j|t} \in \Omega_A, B_{t+j|t} \in \Omega_B} J_\infty^1(t) < V(1,t)$$

Therefore, problem (15) is equivalent to the following one:

$$\begin{aligned} \min_{\bar{u}(t|t), \bar{u}(t+i|t), i=1,2,\dots} \quad &x(t|t)^T W x(t|t) + \bar{u}(t|t)^T R \bar{u}(t|t) \\ &+ x(t+1|t)^T P(1,t)x(t+1|t) \\ \text{s.t. (11), (12), (20), } \quad &-\Delta \underline{u} \leq \bar{u}(t+i|t) \leq \Delta \bar{u}, \quad i \geq 0 \quad (21) \end{aligned}$$

If there exist the Lyapunov matrices  $P_{ik}$  ( $i,k = 1,2,\dots,L_h$ ) which is applied to build a time-varying parameter-dependent Lyapunov matrix:

$$P(j,t) = \sum_{i=1}^{L_h} \alpha_i(t+j|t) \sum_{k=1}^{L_h} \beta_k(t+j|t) P_{ik} \quad (22)$$

Problem (21) can then be solved as showed in Theorem 1.

**Theorem 1.** The optimization problem (21) with the control law (18) can be solved by the following semi-definite programming:

$$\min_{\gamma, \bar{u}(t|t), Y, G, Q_{ik}, Z} \gamma \quad (23)$$

Subject to

$$\begin{bmatrix} 1 & * & * & * \\ A_t x(t|t) + B_t \bar{u}(t|t) + \Xi(t) & Q_{ik} & * & * \\ W^{1/2} x(t|t) & 0 & \gamma I & * \\ R^{1/2} \bar{u}(t|t) & 0 & 0 & \gamma I \end{bmatrix} \geq 0 \quad (24)$$

$$\begin{bmatrix} G + G^T - Q_{ik} & * & * & * \\ A_l G + B_k Y & Q_{ef} & * & * \\ W^{1/2} G & 0 & \gamma I & * \\ R^{1/2} Y & 0 & 0 & \gamma I \end{bmatrix} \geq 0 \quad (25)$$

$$i, k, e, f = 1, 2, \dots, L_h \quad (26)$$

$$-\Delta \underline{u} \leq \bar{u}(t|t) \leq \Delta \bar{u}$$

$$\begin{bmatrix} Z & Y \\ Y^T & G + G^T - Q_{ik} \end{bmatrix} \geq 0, \quad Z_{jj} \leq [\min\{\Delta \underline{u}, \Delta \bar{u}\}]^2 \quad (27)$$

where the symbol  $*$  induces a symmetric structure,  $P_{ik} = \gamma Q_{ik}^{-1} > 0$ ,  $Z$  is a symmetric matrix and the feedback gain is given by  $F(t) = YG^{-1}$ .

*Proof:* Introducing (12), (18) and (19) into (20), one can get

$$x(t+j|t)^T \begin{cases} [A_{t+j|t} + B_{t+j|t} F(t)]^T P(j+1,t) \\ \times [A_{t+j|t} + B_{t+j|t} F(t)] \\ - P(j,t) + F(t)^T RF(t) + W \end{cases} x(t+j|t) \leq 0 \quad (28)$$

That is satisfied for all  $j \geq 1$  if

$$\begin{aligned} &[A_{t+j|t} + B_{t+j|t} F(t)]^T P(j+1,t) [A_{t+j|t} + B_{t+j|t} F(t)] \\ &- P(j,t) + F(t)^T RF(t) + W \leq 0 \end{aligned} \quad (29)$$

It is easy to be confirmed that inequality (29) is satisfied if and only if there exists  $n \cdot k_n \times n \cdot k_n$  symmetric positive matrices  $P_{ik}$  ( $i,k = 1,2,\dots,L_h$ ) such that the time-varying parameter-dependent Lyapunov matrix  $P(j,t)$  is obtained by (22), and

$$[A_i + B_k F(t)]^T P_{ef} [A_i + B_k F(t)] - P_{ik} + F(t)^T RF(t) + W \leq 0 \quad (30)$$

Furthermore, define  $F(t) = YG^{-1}$ ,  $Q_{ik} = \gamma P_{ik}^{-1}$ , and  $Q_{ef} = \gamma P_{ef}^{-1}$  ( $i,k,e,f = 1,2,\dots,L_h$ ). By using Schur complement, inequality (30) can be expressed as LMIs (25). Minimization problem (21) is now equivalent to

$$\min_{\gamma, \bar{u}(t|t), Y, G, Q_{ik}} \gamma$$

Subject to (11), (25),  $-\Delta \underline{u} \leq \bar{u}(t+i|t) \leq \Delta \bar{u}$ ,  $i \geq 0$ , and

$$\begin{aligned} &x(t|t)^T W x(t|t) + \bar{u}(t|t)^T R \bar{u}(t|t) \\ &+ x(t+1|t)^T P(1,t)x(t+1|t) \leq \gamma \end{aligned} \quad (31)$$

Introducing (11) into (31), and according to (22), the resulted inequality is equivalent to the following one:

$$\begin{aligned} &[A_t x(t|t) + B_t \bar{u}(t|t) + \Xi(t)]^T P_{ik} [A_t x(t|t) + B_t \bar{u}(t|t) + \Xi(t)] \\ &+ x(t|t)^T W x(t|t) + \bar{u}(t|t)^T R \bar{u}(t|t) \leq \gamma \end{aligned} \quad (32)$$

By using Schur complement and noting that  $P_{ik} = \gamma Q_{ik}^{-1}$  ( $i,k = 1,2,\dots,L_h$ ), inequality (32) can be expressed as LMIs (24). Furthermore, referring to [7], it is clear that the input constraint  $-\Delta \underline{u} \leq \bar{u}(t+i|t) \leq \Delta \bar{u}$ ,  $i \geq 1$  is met if LMIs (27) are satisfied. Therefore, one can conclude that minimization problem (31) is finally equivalent to  $\min_{\gamma, \bar{u}(t|t), Y, G, Q_{ik}, Z} \gamma$ , subject to (24,25,26,27).  $\square$

On the basis of the conclusion showed in Theorem 1, the following result analogous to Lemma 2 and Theorem 3 in [5] may be obtained:

**Theorem 2.** Assume that the LMI optimization problem (23) admits a solution at time  $t$ .

- 1) Then it admits a solution for all future instants.
- 2) The feasible receding horizon control law obtained from Theorem 1 robustly asymptotically stabilizes the closed-loop system represented by (11) and (12).  $\square$

#### IV. CASE STUDY

A thermal power plant simulation of a 600MW sliding pressure type boiler-turbine system [11] created in MATLAB SIMULINK is used as the plant to be controlled in this paper. This simulation plant is based on a set of physical models designed in accordance with operational and physical data of an actual plant and includes a total of 40 variables. The model is not linearized near equilibrium, and can imitate the strong nonlinear dynamic properties of power systems under large load variations. In this simulation model, sets of conventional multi-loop gain-scheduling PID regulators are also used to control the power plant as would be common in practice. Fig. 1 shows the block diagram of the simulation plant created in MATLAB SIMULINK.

The gain-scheduling PID controllers and the MIMO RBF-ARX model-based min-max robust nonlinear MPC (RBF-ARX-Min-Max-MPC) presented in this paper operate in parallel in the proposed control system. The outputs and the inputs of the controlled plant are given as follows

$$y(t) = \begin{bmatrix} y_1(t) : \text{STE (main steam temperature error / } ^\circ\text{C)} \\ y_2(t) : \text{RTE (reheat steam temperature error / } ^\circ\text{C)} \\ y_3(t) : \text{TPE (main steam pressure error / bar)} \end{bmatrix}$$

$$u(t) = \begin{bmatrix} u_1(t) : \text{FFI (fuel flow increment)} \\ u_2(t) : \text{1SPI (1st stage spray flow increment)} \\ u_3(t) : \text{2SPI (2st stage spray flow increment)} \\ u_4(t) : \text{GRI (flue gas recirculation flow increment)} \\ u_5(t) : \text{TCI (turbine control increment)} \end{bmatrix}$$

The sampling interval in the MPC is 30 seconds. For safe and economical operation of the plant, the errors of the output variables,  $y(t)$ , should be controlled to be as near to zero as possible, whatever the load level. This system being controlled is nonlinear, and has the dynamic features depending on the time-varying load demand  $w(t)$  of the power plant [11]. This provides a justification for using a load-dependent MIMO RBF-ARX model (33) to describe the nonlinear dynamics of thermal power plants, which is given by

$$\begin{aligned} y(t) &= \phi_0(\bar{w}(t-1)) + \sum_{i=1}^{k_a} \phi_{y,i}(\bar{w}(t-1))y(t-i) \\ &\quad + \sum_{i=1}^{k_b} \phi_{u,i}(\bar{w}(t-1))u(t-i) + \xi(t) \\ \phi_0(\bar{w}(t-1)) &= c_0^0 + \sum_{k=1}^h c_k^0 \exp\left\{-\|\bar{w}(t-1) - z_{y,k}\|_{\lambda_{y,k}}^2\right\} \quad (33) \\ \phi_{j,i}(\bar{w}(t-1)) &= c_{i,0}^j + \sum_{k=1}^h c_{i,k}^j \exp\left\{-\|\bar{w}(t-1) - z_{j,k}\|_{\lambda_{j,k}}^2\right\} \\ \bar{w}(t-1) &= [w(t-1) \quad w(t-2) \quad \dots \quad w(t-n_w)]^\top \\ z_{j,k} &= [z_{j,k,1} \quad z_{j,k,2} \quad \dots \quad z_{j,k,n_w}]^\top, \quad j = y, u \end{aligned}$$

where the load demand sequence  $\bar{w}(t-1) \in \mathbb{R}^{n_w}$  of the power plant is utilized for describing the working-point state of the system.

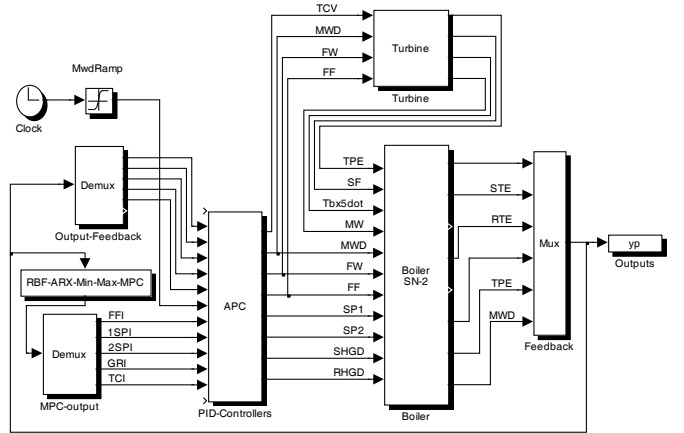


Fig. 1. Diagram of the simulation plant built by MATLAB SIMULINK.

Fig. 2 shows the estimated model residuals and the comparison between the actual data and data generated by the fitted MIMO-RBF-ARX model (33), where the plant inputs were a set of independent PRBS signals with unit amplitude, from which it is clear that the MIMO RBF-ARX model provides a very close fit to the actual data. The structured nonlinear parameter optimization method (SNPOM) [15] is used for estimating model (33), and the model orders selected in this case study are  $k_a = 3$ ,  $k_b = 3$ ,  $h = 1$ ,  $n_w = 2$ . Figs. 3-4 give the simulation results showing the comparison between the estimated MIMO RBF-ARX model (33) based min-max robust MPC proposed and the PID control alone, where  $W = I$ ,  $R = 35I$ . From Fig. 3 one can see that the control performance of the MIMO RBF-ARX model-based NMPC to the simulator of thermal power plants is largely improved as compared with the PID control alone.

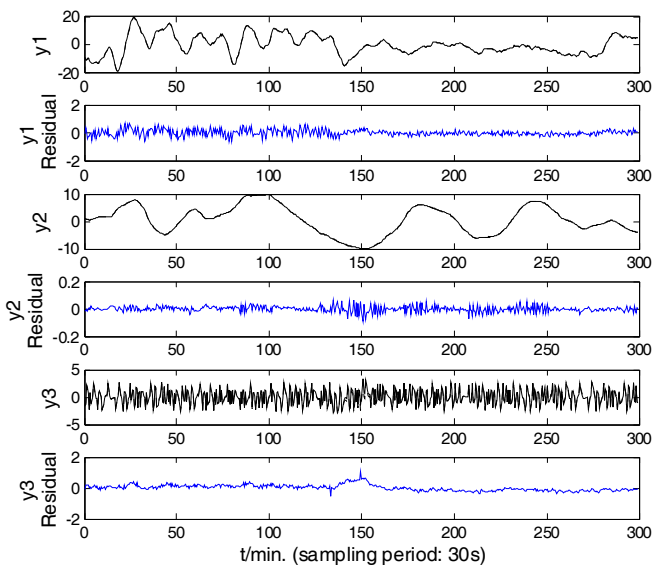


Fig. 2. Model residuals and Comparison between actual outputs (solid line) and model outputs (dotted line) while load changes through the range 40% to 90%.

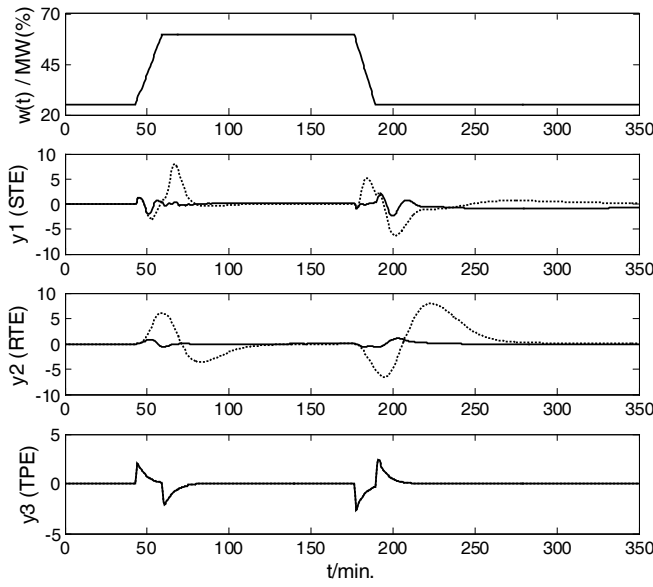


Fig. 3. Comparison of control performance provided by MIMO-RBF-ARX model-based min-max robust MPC (solid line) and PID alone (dotted line).

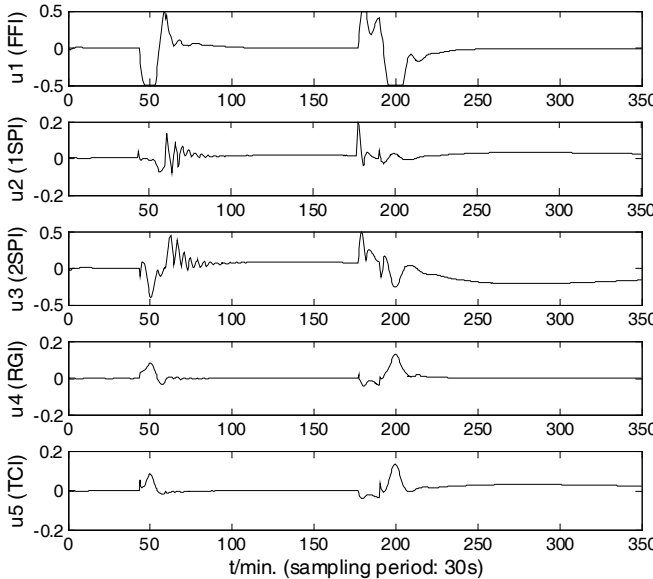


Fig. 4. Control inputs provided by MIMO-RBF-ARX model-based nonlinear robust MPC,  $-0.5 \leq u_i \leq 0.5$ .

## V. CONCLUSION

Based on the offline estimated MIMO RBF-ARX model which could globally represent nonlinear behavior of the underlying system, a local linearized model and a polytopic uncertain linear parameter-varying model could be built to approximate the present and the future system's nonlinear behavior respectively. The built models-based min-max robust nonlinear MPC algorithm proposed in this work did not need to know system steady state; hence, it could be

applied to the nonlinear output-tracking problem with unknown steady state. The closed-loop stability was guaranteed by the use of time-varying parameter-dependent Lyapunov function and the feasibility of the linear matrix inequalities. Case study demonstrated the effectiveness of the modeling and robust MPC approaches proposed.

## ACKNOWLEDGMENT

H. Peng thanks Professor T. Ozaki very much, who invited him to visit the Institute of Statistical Mathematics, Tokyo, Japan, where some previous works related to this paper had been completed.

## REFERENCES

- [1] M. Mahfouf, and D. A. Linkens, "Non-linear generalized predictive control (NLGPC) applied to muscle relaxant anaesthesia," *Int. J. of Control.*, vol. 71, pp. 239-257, 1998.
- [2] G. Sentoni, O. Agamennoni, A. Desages and J. Romagnoli, "Approximate models for nonlinear process control," *AICHE Journal*, vol. 42, pp. 2240-2250, 1996.
- [3] H. H. J. Bloemen, T. J. J. Van Den Boom, and H. B. Verbruggen, "Model-based predictive control for Hammerstein-Wiener systems," *Int. J. of Control.*, vol. 74, pp. 482-485, 2001.
- [4] G. Prasad, E. Swidenbank, and B. W. Hogg, "A local model networks based multivariable long-range predictive control strategy for thermal power plants," *Automatica*, vol. 34, pp. 1185-1204, 1998.
- [5] M. V. Kothare, V. Balakrishnan, and M. Morari, "Robust constrained model predictive control using linear matrix inequalities," *Automatica*, Vol. 32, pp. 1361-1379, 1996.
- [6] Y. Lu, and Y. Arkun, "A scheduling quasi-min-max model predictive control algorithm for nonlinear systems," *J. of Process Control*, vol. 12, pp. 589-604, 2002.
- [7] F. A. Cuzzola, J. C. Gerome and M. Morari, "An improved approach for constrained robust model predictive control," *Automatica*, vol. 38, pp. 1183-1189, 2002.
- [8] D. Q. Mayne, J. B. Rawlings, C. V. Rao and P. O. M. Scokaert, "Constrained model predictive control: Stability and optimality," *Automatica*, vol. 36, pp. 789-814, 2000.
- [9] Z. Lakhdari, M. Mokhtari, Y. Lécluse, and J. Provost, "Adaptive predictive control of a class of nonlinear systems – A case study," in *IFAC Proc.: Adaptive Systems in Control and Signal Processing*, Budapest, Hungary, 1995, pp. 209-214.
- [10] H. Peng, T. Ozaki, V. Haggan-Ozaki, and Y. Toyoda, "A parameter optimization method for the radial basis function type models," *IEEE Trans. Neural Networks*, vol. 14, pp. 432-438, 2003.
- [11] H. Peng, T. Ozaki, V. Haggan-Ozaki, and Y. Toyoda, "A nonlinear exponential ARX model-based multivariable generalized predictive control strategy for thermal power plants," *IEEE Trans. Control Systems Technology*, vol. 10, pp. 256-262, 2002.
- [12] H. Peng, T. Ozaki, K. Nakano, V. Haggan-Ozaki, and Y. Toyoda, "Stability analysis of the RBF-ARX model based nonlinear predictive control," in *Proc. of the European Control Conference (ECC2003)*, Cambridge, UK, 2003.
- [13] H. Peng, T. Ozaki, M. Mori, H. Shioya, and V. Haggan-Ozaki, "Modeling and control of nonlinear nitrogen oxide decomposition process," in *Proc. of IEEE 42<sup>nd</sup> Int. Conf. Decision and Control (CDC'03)*, Hawaii, USA, 2003, pp. 4770-4775.
- [14] H. Peng, T. Ozaki, Y. Toyoda, H. Shioya, K. Nakano, V. Haggan-Ozaki, and M. Mori, "RBF-ARX model based nonlinear system modeling and predictive control with application to a NO<sub>x</sub> decomposition process," *Control Engineering Practice*, vol. 12, pp. 191-203, 2004.
- [15] H. Peng, W. Gui, R. Zou, R. Youssef, and Z. J. Yang, "Nonlinear system modeling and predictive control based on multivariable RBF-ARX model," In *Proc. of IEEE Int. Conf. Control Applications (CCA'05)*, 2005, to be submitted.